Received: 11 August 2022 | Revised: 8 December 2022 | Accepted: 20 December 2022

DOI: 10.1111/cas.15708

Cancer Science WILEY

ORIGINAL ARTICLE

KIAA1429 promotes infantile hemangioma regression by facilitating the stemness of hemangioma endothelial cells

Luying Wang[1] | Yuqing Zou[1] | Zhishun Huang[2,3] | Wenjing Wang[1] | Jing Li[2] | Jianhai Bi[1,2,3] | Ran Huo[1,2,3]

[1]Department of Burn and Plastic Surgery, Shandong Provincial Hospital, Cheeloo College of Medicine, Shandong University, Jinan, China

[2]Department of Burn and Plastic Surgery, Shandong Provincial Hospital Affiliated to Shandong First Medical University, Jinan, China

[3]Medical Science and Technology Innovation Center, Shandong First Medical University & Shandong Academy of Medical Sciences, Taian, China

Correspondence
Ran Huo, Department of Burn and Plastic Surgery, Shandong Provincial Hospital, No. 324, Jing Wu Road 250021, Jinan, China.
Email: huoran@email.sdu.edu.cn

Jianhai Bi, Department of Burn and Plastic Surgery, Shandong Provincial Hospital, No. 324, Jing Wu Road 250021, Jinan, China.
Email: bijianhai@126.com

Funding information
Clinical Medical Science Innovation Program of Jinan, Grant/Award Number: 202019076; National Natural Science Foundation of China, Grant/Award Number: 82172227

Abstract

Infantile hemangiomas are common vascular tumors with a specific natural history. The proliferation and regression mechanism of infantile hemangiomas may be related to the multilineage differentiation ability of hemangioma stem cells, but the specific mechanism is not well elucidated. KIAA1429 is an N^6-methyladenosine methylation-related protein that can also exert its role in a methylation-independent manner. This study aims to explore the function of KIAA1429 in infantile hemangiomas. qRT-PCR, western blotting, and immunostaining were performed to verify the expression of KIAA1429. The endothelial and fibroblast-like phenotypes of hemangioma endothelial cells were detected after KIAA1429 knockdown and overexpression. The stemness properties of hemangioma endothelial cells and the underlying mechanism of KIAA1429 in hemangiomas were also investigated. Nude mouse models of infantile hemangiomas were conducted to ascertain the effects of KIAA1429 in vivo. The results showed that KIAA1429 was highly expressed in infantile hemangiomas, particularly in involuting hemangiomas. In vitro experiments confirmed that KIAA1429 inhibited the endothelial phenotype, enhanced the differentiation ability, and promoted the fibroblast-like phenotype of hemangioma endothelial cells by inducing endothelial cell transition to facultative stem cells. However, the effect of KIAA1429 on the potential target was shown to be independent of N^6-methyladenosine methylation modification. Mouse models further revealed that KIAA1429 could inhibit the proliferation and promote the regression of hemangiomas. In conclusion, this study found that KIAA1429 played an important role in the regression of infantile hemangiomas

Abbreviations: α-tubulin, tubulin Alpha 1a; β-actin/*ACTB*, homo sapiens actin beta; CD31/*PECAM1*, platelet endothelial cell adhesion molecule-1; *CDH5*, VE-Cadherin; *COL1A1*, collagen type I alpha 1 chain; *COL3A1*, collagen type III alpha 1 chain; collagen-I, collagen type I; collagen-III, collagen type III; ECGS, endothelial cell growth supplement; ECM, endothelial cell medium; *ENG*, endoglin; EV, empty vector; *FN1*, fibronectin; GLUT1/*SLC2A1*, glucose transporter 1; HemECs, hemangioma endothelial cells; HemSCs, hemangioma stem cells; HFF-1, human foreskin fibroblasts; HIF1α/*HIF1A*, hypoxia inducible factor 1 alphahypoxia inducible factor 1 alpha; HMEC-1, human microvascular endothelial cells; HUVECs, human umbilical vein endothelial cells; IF, immunofluorescence; IHC, immunohistochemistry; IHs, infantile hemangiomas; m^6A N^6, methyladenosine methylation; MVD, microvessel density; OE-KIAA1429, KIAA1429 overexpression vector; qRT-PCR, reverse-transcription quantitative PCR; RIP, RNA immunoprecipitant; *S100A4*, S100 Calcium Binding Protein A4; *SERPINH1*, Serpin Family H Member 1; shKIAA1429, KIAA1429 shRNA; shNC, normal control shRNA; αSMA/*ACTA2*, alpha smooth muscle actin; VEGFA, vascular endothelial growth factor A; VEGFR2/*KDR*, vascular endothelial growth factor receptor 2; *VIM*, vimentin; *VIRMA*, vir such as m^6a methyltransferase associated; vWF, von Willebrand factor.

Yuqing Zou, Zhishun Huang, Jianhai Bi and Ran Huo contributed equally to this study.

by enhancing the stemness of hemangioma endothelial cells and could be a potential treatment target for infantile hemangiomas.

KEYWORDS
cell differentiation, endothelial cells, fibroblast, hemangioma, stem cells

1 | INTRODUCTION

Infantile hemangiomas are the most common vascular tumors in infants and can involve the skin, subcutaneous tissues, and even internal organs.[1,2] The natural history of IHs is characterized by spontaneous regression. IHs often proliferate rapidly in the first few weeks of life until 3–6 months, after which the growth rate slows.[1,3] Subsequently, IHs gradually enter a long involuting phase and usually complete their involution by 3 years of age or later.[4] Ulceration, functional disorders, or disfigurement collapse may occur during the rapid proliferative phase, which requires timely intervention.[5,6]

The pathogenesis of IHs remains unclear. It has been established that an imbalance between angiogenic and antiangiogenic factors induced by hypoxia leads to IHs.[1,7] In the proliferative phase, upregulated angiogenic factors result in the abnormal proliferation of HemECs, which form immature microvascular lumens. Subsequently, during the involuting phase, HemECs cease abnormal proliferation, and the lumens begin to expand and mature whereas an increasing number of adipocytes appears. Finally, IHs enter the involuted phase, replacing the tumors with fibrofatty tissue. HemSCs are believed to guarantee this specific course.[8] HemSCs mainly differentiate into HemECs and pericytes during the proliferative phase, but they tend to differentiate into mesenchymal cells with adipogenic potential in the involuting phase.[1] Interestingly, Yu et al. proved that some HemECs can also express stem cell marker CD133.[9] Another study reported that GLUT1-positive ($GLUT1^+$) HemECs exhibited features of facultative stem cells and have adipogenic potential, such as HemSCs.[10] These findings suggest that the regression of IHs is not only dominated by HemSCs, but that HemECs may also play an important role.

As a common post-transcriptional modification, m^6A RNA plays an important role in various tumors.[11] Currently, research into the role of m^6A modification in IHs is limited. KIAA1429, an RNA-binding protein belonging to the m^6A 'writers' complex, is usually reported to be involved in tumor regulation in an m^6A-dependent manner.[12–14] However, some studies have reported that KIAA1429 also functions in an m^6A-independent manner.[15,16] To date, the expression and role of KIAA1429 in IHs have not been explored.

In this study, we verified the expression profile of m^6A-related proteins in IHs using GEO DataSets and found high expression of KIAA1429 in IHs. This expression difference was further confirmed in IHs tissues and HemECs. In addition, we found that KIAA1429 could promote IHs regression in vivo and in vitro, and that this effect was caused by inducing the transition of HemECs to facultative stem cells in an m^6A-independent manner. The results of this study suggest that KIAA1429 may be a potential therapeutic target for IHs.

2 | MATERIALS AND METHODS

2.1 | Tissues collection and cell culture

IHs and normal skin tissue samples were obtained from the Department of Plastic Surgery, Shandong Provincial Hospital with the informed consent of guaranties and the approval of the Committee for Ethical Review of Research involving Human Subjects of Shandong Provincial Hospital (NSFC: no. 2021-743). HemECs and HemSCs were isolated from IHs. In brief, IHs were digested with diapase II (Sigma-Aldrich) and a mixture of collagenase I (Sigma-Aldrich) and DNase (Roche Diagnostics). $CD31^+$ magnetic bead selection (Miltenyi Biotech) and $CD133^+$ magnetic bead selection (Miltenyi Biotech) were used to isolated HemECs and HemSCs, respectively. The isolated HemECs and HemSCs were cultured in ECM (Sciencell) with 5% FBS (Sciencell) and 1% ECGS (Sciencell). The HUVEC cell line (CRL-1730), HMEC-1 cell line (CRL-3243), and HFF-1 cell line (SCRC-1041) were obtained from Shanghai GeneChem.

Other materials and methods used in qRT-PCR, western blotting, IHC staining, IF staining, flow cytometry, cell transfection, CCK-8 assay, transwell assay, wound healing assay, tube formation assay, apoptosis assay, adipogenic differentiation assay, and Oil-Red-O staining, RIP, mRNA stability assay, and animal studies are described in Appendix S1. The primers used in this manuscript are listed in Table S1.

2.2 | Statistics

The data were analyzed using SPSS 25.0 software and GraphPad Prism 8 software. Student's *t* test was performed to evaluate the differences between the two groups. Linear correlation analysis was used to assess the correlation between IHC scores of KIAA1429 and patient age. $^*p<0.05$ was considered a statistically significant difference.

3 | RESULTS

3.1 | KIAA1429 was highly expressed in IHs

GEO DataSets (GSE127487) were analyzed and the results revealed that KIAA1429 and YTHDF1 were highly expressed in IHs (Figure 1A,B). With a more significant fold-change of 2.14, KIAA1429 was further analyzed. The results of qRT-PCR and western blotting analyses verified that KIAA1429 was more highly

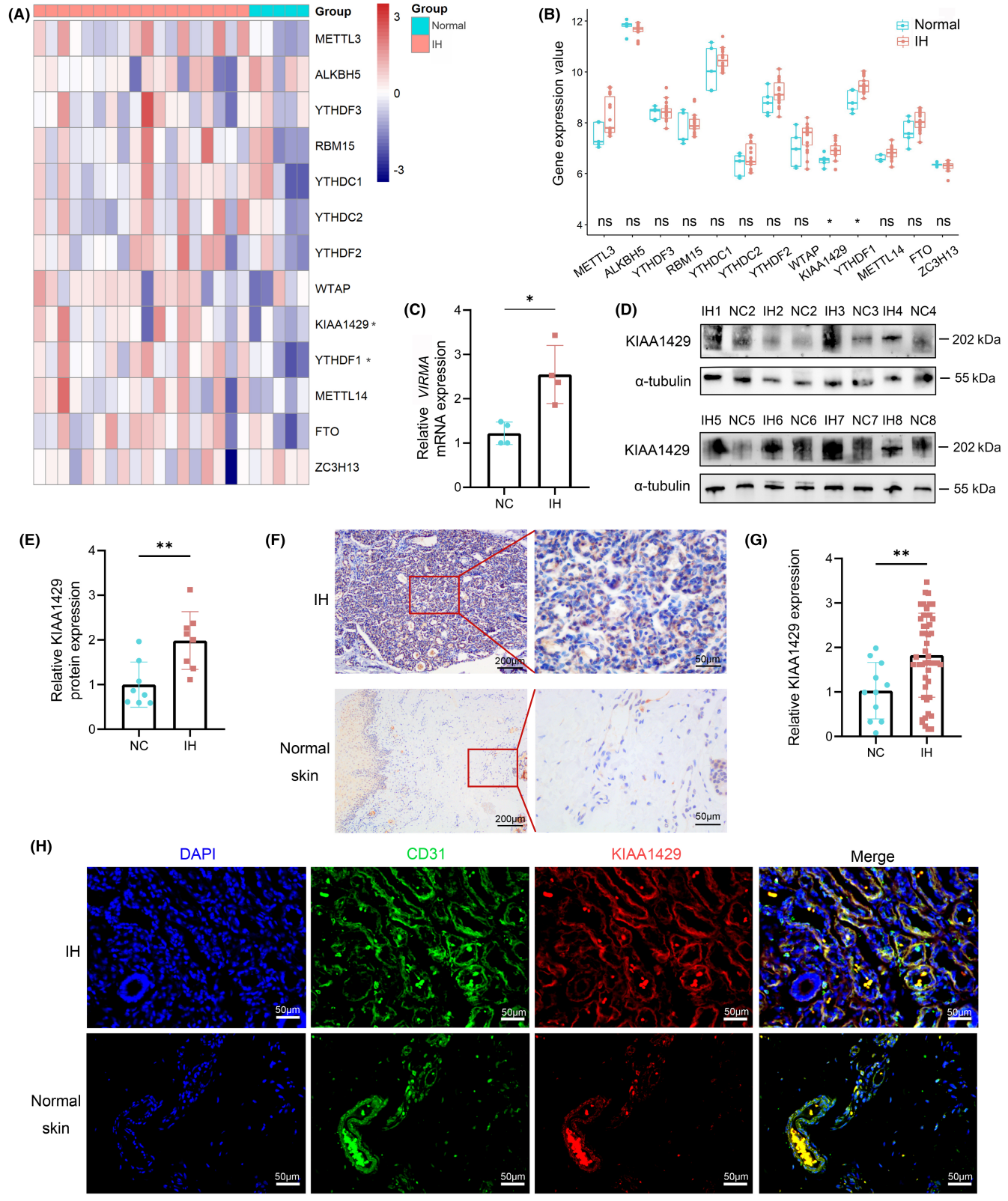

FIGURE 1 KIAA1429 is highly expressed in IHs. Heatmap (A) and scatter plot (B) showing relative transcriptome levels of m^{6}A-related molecules in infantile hemangiomas (IHs) ($n = 18$) and normal skin ($n = 5$). (C) qRT-PCR analysis of *VIRMA* in proliferative IHs and normal skin ($n = 4$). Representative images (D) and scatter plot (E) of western blotting for KIAA1429 expression in proliferative IHs and normal tissue ($n = 8$). Representative images (F) and scatter plot (G) of immunohistochemical staining showing KIAA1429 expression in IHs ($n = 48$) and normal skin ($n = 11$). (H) Representative images of immunofluorescence staining of CD31 and KIAA1429 in IHs and normal skin. Statistical analysis: two-tailed unpaired Student's *t* test for (B) and (G), two-tailed paired Student's *t* test for (C) and (E); $^*p < 0.05$, $^{**}p < 0.01$. NC, normal control; ns, nonsignificant.

expressed in IHs than in normal peritumor skin (Figure 1C–E). IHC staining of 48 IHs and 11 normal skin samples also confirmed that KIAA1429 was highly expressed in IHs compared with normal skin (Figure 1F,G), whereas the positive and negative control images for IHC of KIAA1429 are shown in Figure S1. Moreover, IF with KIAA1429 and CD31 staining also showed this differential expression and identified that the location of KIAA1429 in IHs was mainly in endothelial cells (Figure 1H).

3.2 | KIAA1429 was more highly expressed in involuting IHs

Immunostaining revealed that KIAA1429 was more highly expressed in involuting IHs than in proliferative IHs (Figure 2A). Correlation analysis between the IHC scores of KIAA1429 and patient age showed a positive correlation ($p = 0.019$; Figure 2B). Interestingly, we found that, even for the same IH lesion, the expression of KIAA1429 in the nonproliferative region was higher than that in the proliferative region (Figure 2C). These findings suggest that KIAA1429 may play an important role in IHs regression.

3.3 | KIAA1429 was highly expressed in HemECs

HemECs were isolated, and the morphology is shown in Figure 3A. The cells were identified by flow cytometry detecting CD31 (Figure 3B) and IF staining of CD31, GLUT1, and vWF (Figure 3C). qRT-PCR and western blotting showed that *VIRMA*/KIAA1429 in HemECs was higher than in HUVECs and HMEC-1 (Figure 3D–F), although the difference in qRT-PCR was insignificant. Considering that IHs are often involved in skin tissue, we also compared KIAA1429 expression in HemECs to that in HFF-1 and found that KIAA1429 in HemECs was significantly higher than in HFF-1 (Figure 3D–F). KIAA1429 knockdown and overexpression in HemECs were constructed to explore the effects of KIAA1429 in vitro. The transfection efficiency was verified using fluorescence photography (Figure S2). qRT-PCR and western blotting confirmed the knockdown and overexpression efficiencies (Figure 3G,H). No significant change was observed in cell morphology after the KIAA1429 knockdown (Figure 3I). However, HemECs with KIAA1429 overexpression exhibited fibroblast-like changes, which manifested with long fusiform changes in cell morphology and the flow vortex cell arrangement pattern (Figure 3I).

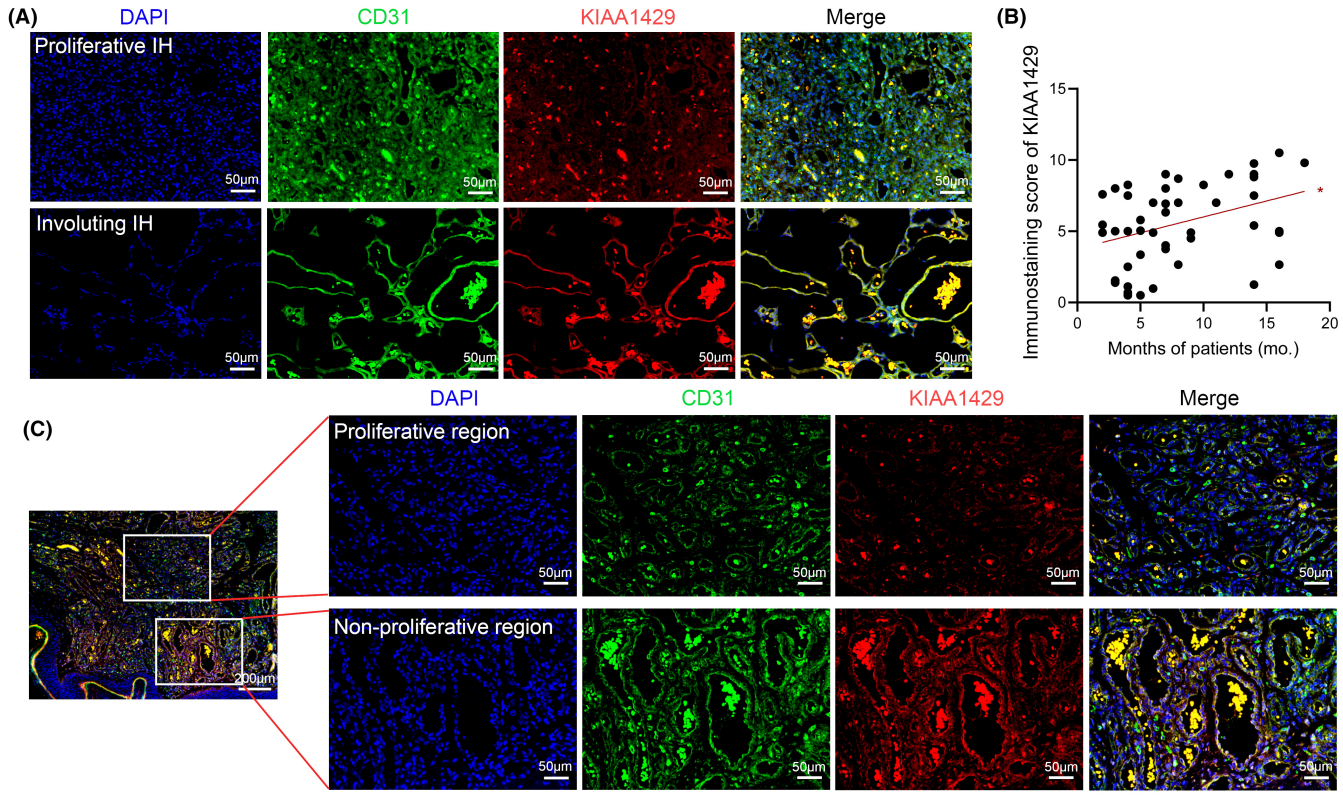

FIGURE 2 KIAA1429 expression was higher in involuting IHs than in proliferative IHs. (A) Representative immunofluorescence staining of CD31 and KIAA1429 in proliferative and involuting IHs. (B) Linear correlation analysis of the immunohistochemical score of KIAA1429 and patient age ($n = 48$). *$p < 0.05$. (C) Representative immunofluorescence staining of CD31 and KIAA1429 in the proliferative and nonproliferative regions of the same IH sample.

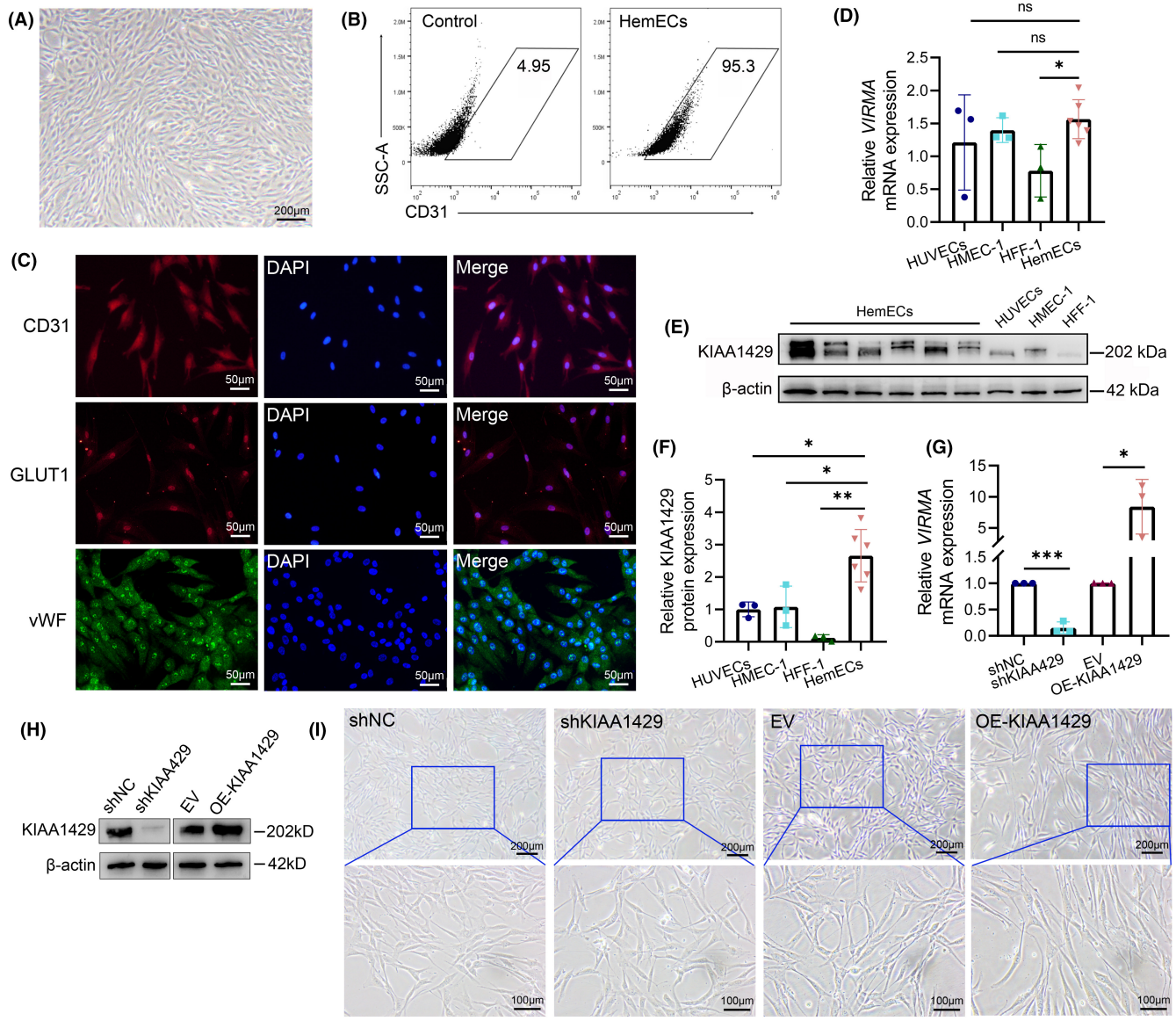

FIGURE 3 The expression and fibroblast-like morphology induction of KIAA1429 in hemangioma endothelial cells (HemECs). (A) The morphologies of HemECs. (B) Representative flow cytometric plot showing the cell purity of HemECs reached 95%. (C) Representative immunofluorescence staining showing the expression of HemEC markers on the sorted cells. (D) qRT-PCR analysis of *VIRMA* in HemECs ($n = 6$), human microvascular endothelial cells (HMEC-1), human foreskin fibroblasts (HFF-1), and human umbilical vein endothelial cells (HUVECs). Representative images (E) and scatter plot (F) of western blotting for KIAA1429 expression in HemECs ($n = 6$), HUVECs, HMEC-1, and HFF-1. (G) qRT-PCR analysis of *VIRMA* in HemECs after transfection with normal control shRNA (shNC), KIAA1429 shRNA (shKIAA1429), empty vector (EV), and KIAA1429 overexpression vector (OE-KIAA1429) viruses ($n = 3$). (H) Representative western blotting for KIAA1429 expression in HemECs after transfection with shNC, shKIAA1429, EV, and OE-KIAA1429 viruses. (I) Morphologies of HemECs after transfection with shNC, shKIAA1429, EV, and OE-KIAA1429 viruses. Statistical analysis: two-tailed unpaired Student's *t* test for (D) and (F), two-tailed paired Student's *t* test for (G); $^{*}p < 0.05$, $^{**}p < 0.01$, $^{***}p < 0.001$. NC, normal control.

3.4 | KIAA1429 weakened the endothelial phenotype of HemECs

CCK-8 assay showed that the proliferation ability of HemECs was enhanced after KIAA1429 knockdown, but decreased after KIAA1429 overexpression (Figure 4A). TUNEL staining revealed that KIAA1429 did not influence apoptosis in HemECs (Figure S3). The cell migration ability was confirmed using a wound healing assay and a transwell migration assay, which showed that the cell migration ability was enhanced after KIAA1429 knockdown but decreased after KIAA1429 overexpression (Figure 4B,C and Figure S4A,B). Transwell invasion assay showed that the invasive ability of HemECs was enhanced after KIAA1429 knockdown, but decreased after KIAA1429 overexpression (Figure 4D,E). Tube formation assay showed that the tube-forming ability was enhanced after KIAA1429 knockdown, but decreased after KIAA1429 overexpression (Figure 4F,G). The transcriptome levels of *VEGFA*, *PECAM1*, *HIF1A*, *KDR*, *ENG*, and *CDH5* were detected by qRT-PCR. The results showed that, after KIAA1429

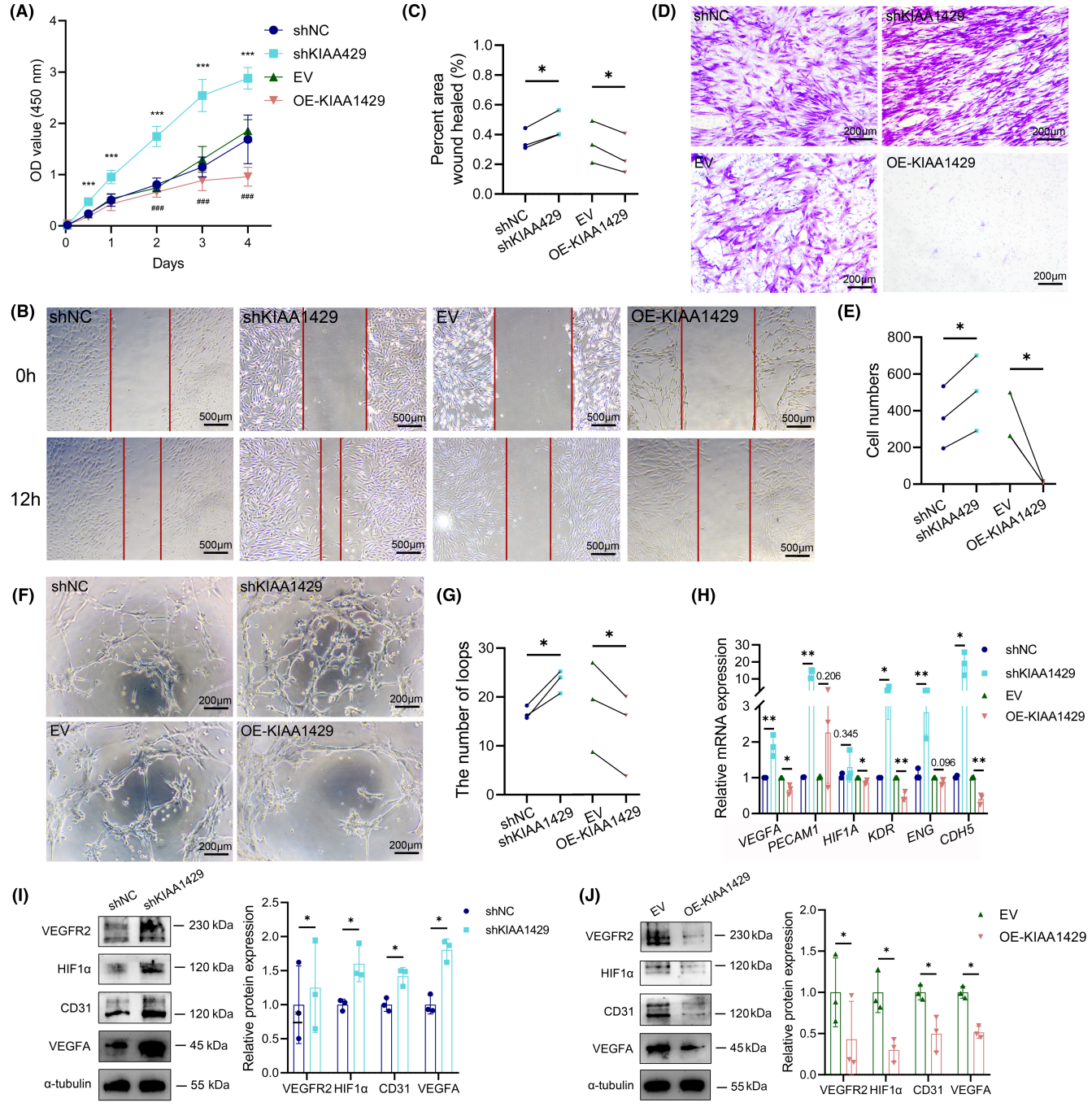

FIGURE 4 KIAA1429 inhibited endothelial phenotype of hemangioma endothelial cells (HemECs). (A) Cell proliferation was evaluated by the CCK-8 assay. Representative images (B) and scatter plot (C) ($n = 3$) of wound healing assay showing the migration ability of HemECs. Representative images (D) and scatter plot (E) ($n = 3$) of transwell invasion assay showing the invasion ability of HemECs. Representative images (F) and scatter plot (G) ($n = 3$) of tube formation assay showing the angiogenesis ability of HemECs. (H) qRT-PCR analysis of endothelial markers (*VEGFA*, *PECAM1*, *HIF1A*, *KDR*, *ENG*, and *CDH5*) in HemECs ($n = 3$). (I) Representative images (left) and scatter plot (right, $n = 3$) of western blotting for endothelial markers (VEGFR2, HIF1α, CD31, and VEGFA) in HemECs after KIAA1429 knockdown. (J) Representative images (left) and scatter plot (right, $n = 3$) of western blotting for endothelial markers (VEGFR2, HIF1α, CD31, and VEGFA) in HemECs after KIAA1429 overexpression. Statistical analysis: two-tailed paired Student's *t* test; $^{*}p < 0.05$, $^{**}p < 0.01$, $^{***}p < 0.001$. EV, empty vector; OE-KIAA1429, KIAA1429 overexpression vector; shKIAA1429, KIAA1429 shRNA; shNC, normal control shRNA.

knockdown, most of the endothelial markers increased, while *HIF1A* increased slightly with no statistical significance (Figure 4H). By contrast, after KIAA1429 overexpression, most of the endothelial markers decreased except *ENG* and *PECAM1* (Figure 4H). Western blotting detected the expression levels of VEGFR2, HIF1α, CD31, and VEGFA. The results showed that these endothelial markers increased after KIAA1429 knockdown and decreased after KIAA1429 overexpression (Figure 4I,J). The inconsistency of protein expression and mRNA

levels in some markers, such as CD31, might be due to the negative feedback caused by the change in protein expression.

3.5 | KIAA1429 enhanced the fibroblast-like phenotype in HemECs

As fibroblast-like changes were observed after KIAA1429 overexpression, we further detected the expression levels of some fibroblast-related factors after knockdown and overexpression of KIAA1429. qRT-PCR showed that the levels of *ACTA2*, *FN1*, *COL1A1*, *COL3A1*, *VIM*, *S100A4*, and *SERPINH1* decreased after KIAA1429 knockdown, while most of these factors increased or tended to increase except *ACTA2* after KIAA1429 overexpression (Figure 5A). As shown by the western blotting results in Figure 5B,C, the expression levels of fibronectin, collagen-III, collagen-I, and αSMA decreased after KIAA1429 knockdown and increased, or had the tendency to increase, after KIAA1429 overexpression. The above results indicated that KIAA1429 decreased the endothelial phenotype, but promoted their transition into the fibroblast-like phenotype of HemECs. We incubated HemECs on noncoated plates and observed the adherence degree after 4 h to further investigate this functional transition of HemECs. The results showed that ~60% of HemECs could stick to the noncoated plates after KIAA1429 overexpression (Figure 5D,E).

3.6 | KIAA1429 induced HemECs differentiation to facultative stem cells

Considering that some HemECs had the characteristics of facultative stem cells,[9,10] we suspected that the changes in HemECs to a fibroblast-like phenotype were caused by the enhanced stemness. Therefore, we examined the adipogenic differentiation ability of HemECs and the expression of CD133 in HemECs. Adipogenic induction showed that the adipogenic differentiation ability of HemECs decreased after KIAA1429 knockdown, but more HemECs differentiated into adipocytes after KIAA1429 overexpression (Figure 5F,G). Moreover, the expression of CD133 decreased after KIAA1429 knockdown, but increased significantly after KIAA1429 overexpression (Figure 5H), which verified the stemness facilitation of KIAA1429 in HemECs directly. The results of weakening of the endothelial phenotype and promotion of endothelial-to-stem cell transition manifested by the fibroblast phenotype and adipogenesis ability from KIAA1429 overexpression were consistent with the specific course of IHs spontaneous regression to fibroadipose tissue, indicating that KIAA1429 could promote IHs regression.

3.7 | KIAA1429 functioned in HemECs in an m^{6}A-independent manner

GLUT1, as a specific HemECs marker, is a proven indicator of facultative stem cells and is related to the specific course of IHs.[10] Therefore, we detected the mRNA and protein expression levels of GLUT1 after KIAA1429 knockdown and overexpression. Interestingly, unlike other endothelial markers, GLUT1 was downregulated after KIAA1429 knockdown, but increased after KIAA1429 overexpression, although the increase in transcriptome level was insignificant (Figure 6A,B). These results were consistent with the change in CD133 expression and stemness enhancement after KIAA1429 overexpression, indicating that KIAA1429 may promote the conversion of HemECs to stem cells via upregulating GLUT1. Considering that KIAA1429 is one component of m^{6}A 'writer' complex, we suspected that its effect on GLUT1 was through m^{6}A modification and performed RIP to confirm this. Western blotting verified the binding efficiency between magnetic beads and KIAA1429 (Figure 6C). However, the RIP results showed that KIAA1429 did not directly target *SLC2A1* (Figure 6D), indicating that KIAA1429 acted on GLUT1 in an m^{6}A-independent manner. As *KDR* and *FN1* might also be the potential target genes, RIP was also conducted on them. Similarly, KIAA1429 did not directly target *KDR* and *FN1* (Figure 6D), suggesting that the KIAA1429 effect on these factors was not mediated by m^{6}A modification. To further confirm the results, mRNA stabilities of potential target genes were detected, and the results showed no significant change in the stabilities of *SLC2A1*, *KDR*, and *FN1* (Figure 6E). Finally, qRT-PCR revealed that KIAA1429 was upregulated after propranolol treatment (Figure 6F), further proving the relationship between KIAA1429 and IHs regression.

3.8 | KIAA1429 promoted the regression of IHs in vivo

The volume of the tumors in mouse models gradually increased in the first 2 weeks and decreased slightly after that (Figure 7A), which was consistent with IH natural history. Tumors were larger in the shKIAA1429 group and smaller in the OE-KIAA1429 group at 2 weeks, although the differences were insignificant (Figure S5A–C). H&E and IF staining showed that endothelial cell masses gathered and formed microvessels in the shNC, shKIAA1429, and EV groups at 2 weeks (Figure 7B,C). In contrast, the OE-KIAA1429 group was mainly comprised of fibroadipose tissue, with a few relatively mature vascular lumens such as involuting IHs (Figure 7B,C). MVD increased after KIAA1429 knockdown, but decreased after KIAA1429 overexpression (Figure 7C,D). qRT-PCR revealed that after KIAA1429 knockdown, the endothelial markers *VEGFA*, *ENG*, and *HIF1A* increased or exhibited an increasing trend, whereas the fibroblast-related markers *COL1A1* and *COL3A1* decreased or showed a downward trend (Figure 7E). In contrast, after overexpression of KIAA1429, *HIF1A* decreased, and *COL1A1* increased (Figure 7E). GLUT1+ vessels were observed by IF staining in each group (Figure 7C). Interestingly, compared with the other three groups, the number of microvessels formed in the OE-KIAA1429 group was lower, but the expression of GLUT1 seemed to be higher, although the difference was insignificant (Figure 7C, F). H&E staining showed that tumors were mainly composed of fibroadipose tissue at 4 weeks, and IF staining for GFP verified that the adipocytes were derived from implanted HemECs (Figure 7G). Moreover, the proportion of adipose tissue in the OE-KIAA1429 group was higher than in the EV group (Figure 7H).

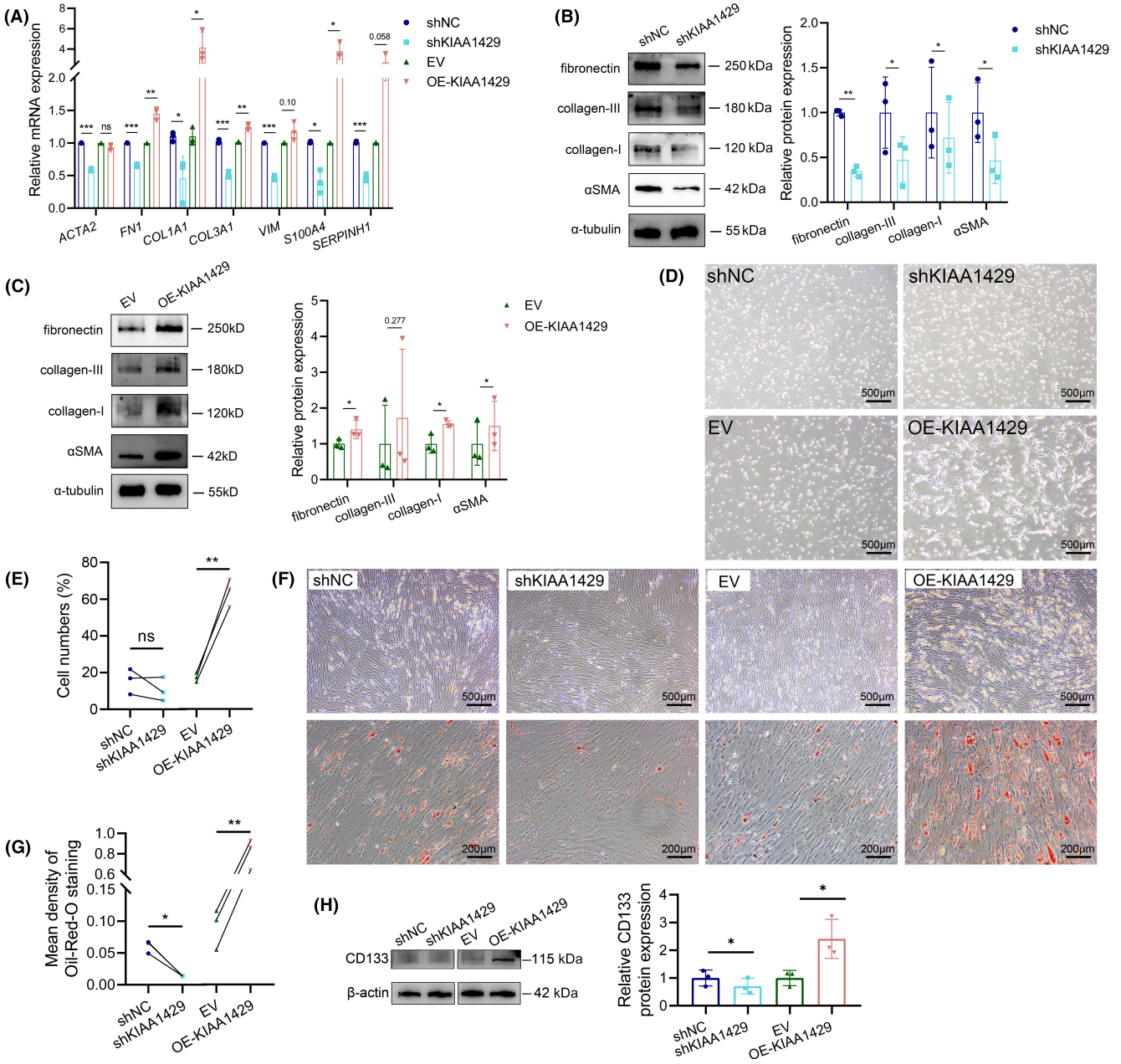

FIGURE 5 KIAA1429 facilitated the fibroblast-like phenotype and enhanced the stemness of hemangioma endothelial cells (HemECs). (A) qRT-PCR analysis of fibroblast-related markers (*ACTA2*, *FN1*, *COL1A1*, *COL3A1*, *VIM*, *S100A4* and *SERPINH1*) in HemECs ($n = 3$). (B) Representative images (left) and scatter plot (right, $n = 3$) of western blotting for fibroblast-related markers (fibronectin, collagen-III, collagen-I and αSMA) in HemECs after KIAA1429 knockdown. (C) Representative images (left) and scatter plot (right, $n = 3$) of western blotting for fibroblast-related markers (fibronectin, collagen-III, collagen-I and αSMA) in HemECs after KIAA1429 overexpression. Representative images of cell morphology (D) and scatter plot of adhesive cells numbers (E) ($n = 3$) after inoculating HemECs to noncoated plates. Representative images (F) and scatter plot (G) of Oil-Red-O staining after adipogenic differentiation induction. (H) Representative images (left) and scatter plot (right, $n = 3$) of western blotting for CD133 in HemECs. Statistical analysis: two-tailed paired Student's *t* test; $^{*}p < 0.05$, $^{**}p < 0.01$, $^{***}p < 0.001$. EV, empty vector; ns, nonsignificant; shKIAA1429, KIAA1429 shRNA; shNC, normal control shRNA; OE-KIAA1429, KIAA1429 overexpression vector.

4 | DISCUSSION

As the most common soft tissue tumor in infants, the incidence of IHs can reach 4–10%.[1,3] In the past, vascular abnormalities were not clearly classified and were often collectively referred to as hemangiomas. In 1982, Mulliken et al. classified vascular abnormalities into vascular tumors and vascular malformations according to whether the abnormal proliferation of endothelial cells existed, and IHs were the most common type in vascular tumors.[17] A well described natural history is characteristic of IHs. Although IHs regress spontaneously, there are ~10–15% of patients with complications such as bleeding, ulceration, compression of functional organs, or disfigurement due

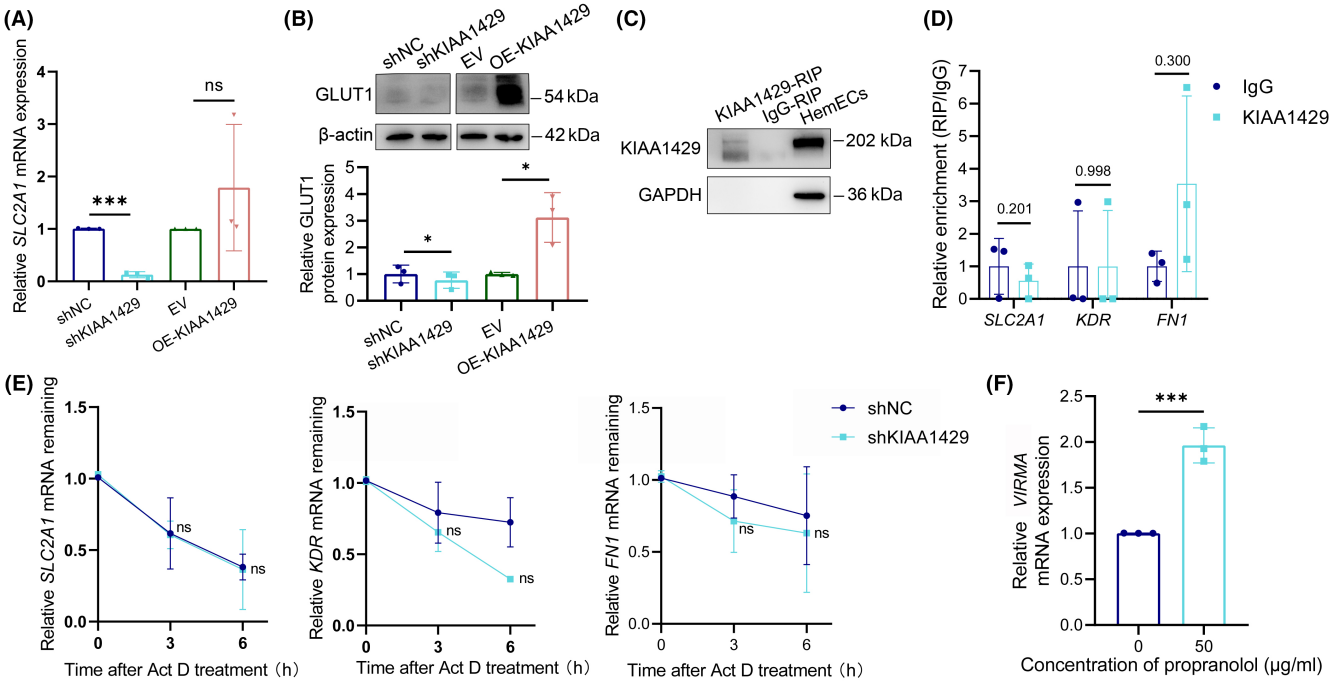

FIGURE 6 KIAA1429 functions in hemangioma endothelial cells (HemECs) independently of N^6-methyladenosine methylation modification. (A) qRT-PCR analysis of *SLC2A1* in HemECs ($n = 3$). (B) Representative images (above) and scatter plot (below, $n = 3$) of western blotting for GLUT1 in HemECs. (C) Western blotting verified the combination of magnetic bead and antibody complex with KIAA1429. (D) qRT-PCR analysis detected the enrichment of *SLC2A1*, *KDR*, and *FN1* normalized with IgG ($n = 3$). (E) mRNA stabilities of *SLC2A1*, *KDR*, and *FN1* after KIAA1429 knockdown ($n = 3$). (F) qRT-PCR analysis of *VIRMA* in HemECs after treatment with propranolol ($n = 3$). Statistical analysis: two-tailed paired Student's *t* test; $^*p < 0.05$, $^{***}p < 0.001$. EV, empty vector; ns, nonsignificant; shKIAA1429, KIAA1429 shRNA; shNC, normal control shRNA; OE-KIAA1429, KIAA1429 overexpression vector; RIP, RNA-immunoprecipitation.

to the rapid growth in IHs.[5,18,19] Therefore, active and timely interventions must be urgently adopted for these patients. Propranolol was accidentally discovered by Léauté-Labrèze in 2008 to treat IHs, and later became first-line treatment, with an average effective rate of up to 90%.[20–22] However, 20–30% of patients relapse after propranolol withdrawal.[23–25] In addition, approximately 10% of IHs patients are propranolol resistant.[26] Therefore, it is important to explore the pathogenesis of IHs and identify other possible therapeutic targets. HemSCs are the basics of IHs and can differentiate into endothelial progenitor cells, hematopoietic stem cells, and mesenchymal stem cells in different phases of IHs.[3,27–30] In the early stage of IHs, the upregulated HIF1α caused by hypoxia and the subsequent upregulation of various angiogenic factors seem to be the reason for IH rapid proliferation.[31] Many pathways and the renin–angiotensin system are involved in this process.[7,32] Later, in the involuting phase, HemSCs are more likely to differentiate into mesenchymal stem cells and then into pericytes and adipocytes, promoting IHs regression.[30] Nevertheless, to date, no hypothesis can fully explain the reasons for the specific course of IHs, especially the reasons for regression.

m^6A is proven to be associated with the pathogenesis and angiogenesis of many tumors.[11,33–35] However, the function of m^6A in IHs has not been discussed much. In this study, we found a high expression of KIAA1429 in IHs in the initial database screening and confirmed KIAA1429 tissue localization. In in vitro experiments, the fibroblast-like morphological changes of HemECs after KIAA1429 overexpression suggested that differentiation induced by KIAA1429 might exist. Previous studies highlighted that HemECs differ from general endothelial cells but resemble fetal endothelial cells.[36,37] Approximately 0.1–2% of HemECs express the stem cell marker CD133, so it is also considered an intermediate form during the transition of HemSCs into endothelial cells.[9] In this study, the weakening of endothelial phenotype and promotion of endothelial-to-stem cell transition manifested by the fibroblast phenotype and adipogenesis ability brought about by KIAA1429 overexpression, were consistent with the spontaneous regression of IHs to fibroadipose tissue, indicating that KIAA1429 could promote IH regression. In animal studies, KIAA1429 inhibited microvessel formation and promoted the progress of regression, further confirming the effect of KIAA1429 in vivo. What is more, the upregulation of KIAA1429 after propranolol treatment suggested that the direct targeting of KIAA1429 would be more effective in patients with propranolol resistance or relapse, although this hypothesis needs to be confirmed in additional studies.

Some studies have revealed that $GLUT1^+$ HemECs, which differ from $GLUT^-$ HemECs, possess the characteristics of facultative stem cells and can re-differentiate into pericytes, smooth muscle cells, and adipocytes.[8,10] We found that KIAA1429 upregulated the expression of GLUT1, which explains why KIAA1429 enhanced the stemness of HemECs to some extent. GLUT1 is a specific marker that distinguishes IHs from other vascular abnormalities.[38] It can be expressed in IHs and 20–30% of angiosarcomas, but not in other vascular tumors.[39]

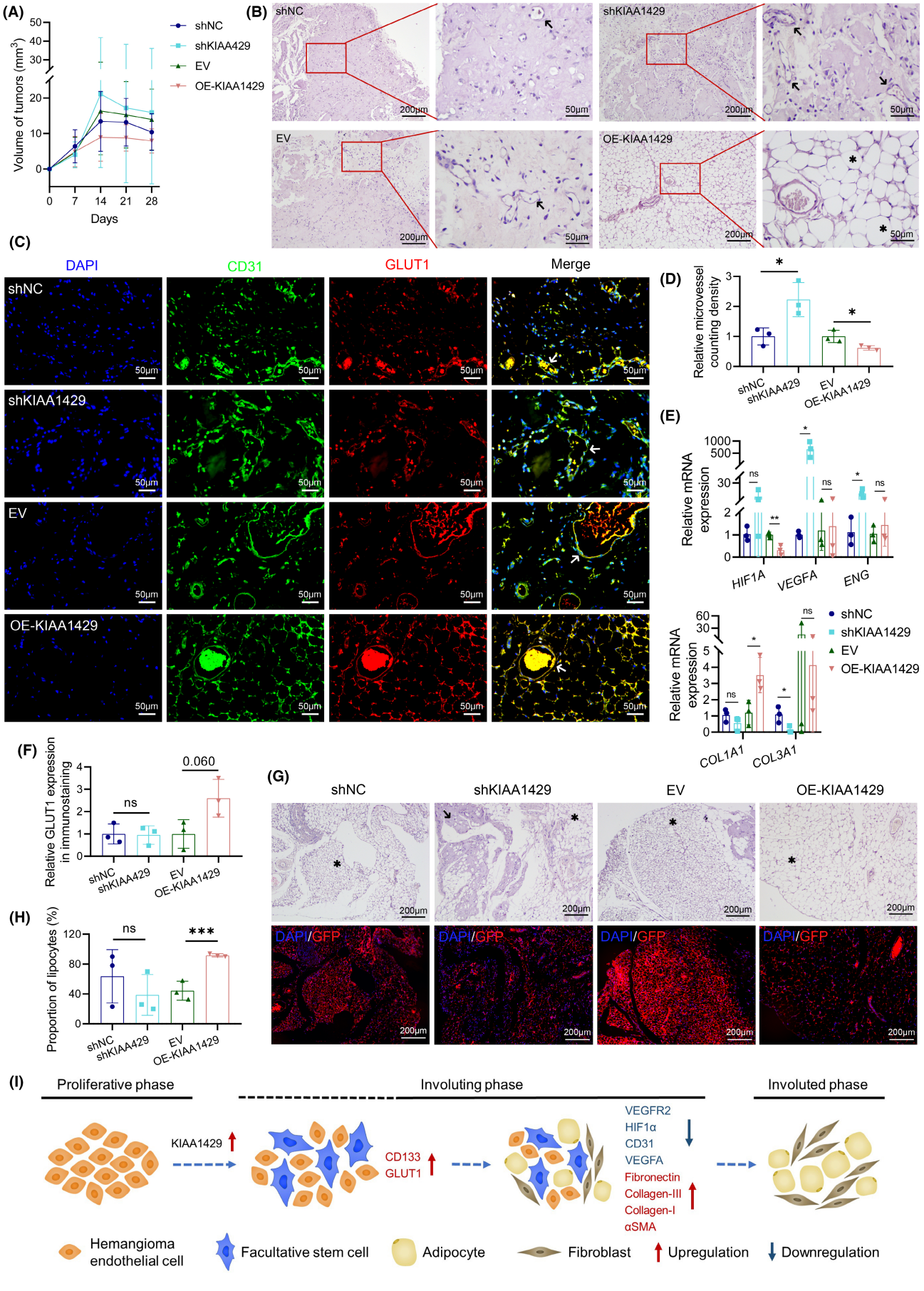
(A)
Volume of tumors (mm3)
Days
shNC
shKIAA429
EV
OE-KIAA1429
(B)
shNC
shKIAA1429
EV
OE-KIAA1429
200μm
50μm
(C)
DAPI
CD31
GLUT1
Merge
50μm
(D)
Relative microvessel counting density
(E)
Relative mRNA expression
HIF1A
VEGFA
ENG
COL1A1
COL3A1
(F)
Relative GLUT1 expression in immunostaining
0.060
ns
(G)
DAPI/GFP
(H)
Proportion of lipocytes (%)
***
(I)
Proliferative phase
Involuting phase
Involuted phase
KIAA1429
CD133
GLUT1
VEGFR2
HIF1α
CD31
VEGFA
Fibronectin
Collagen-III
Collagen-I
αSMA
Hemangioma endothelial cell
Facultative stem cell
Adipocyte
Fibroblast
Upregulation
Downregulation

FIGURE 7 KIAA1429 promoted IHs regression in vivo. (A) Volume changes of tumors within 4 weeks ($n = 8$ for the first 2 weeks and $n = 3$ for the last 2 weeks). (B) Representative H&E staining of tumors at 2 weeks. Arrows pointed to the microvessels, and stars pointed to the adipocytes. (C) Representative immunofluorescence staining of CD31 and GLUT1 of tumors at 2 weeks. Arrows pointed to the microvessels. (D) Microvessel density analyses of tumors at 2 weeks ($n = 3$). (E) qRT-PCR analysis of endothelial markers *HIF1A*, *VEGFA*, *ENG* (upper), and fibroblast-related markers *COL1A1*, *COL3A1* (below) of tumors at 2 weeks ($n = 3$). (F) Scatter plot of the expression levels of GLUT1 in tumors at 2 weeks according to immunostaining ($n = 3$). (G) Representative H&E staining and immunofluorescence staining of GFP for tumors at 4 weeks. The arrows point to the region that had not yet been involuted, and stars point to the adipocytes. (H) The proportion of adipose tissue of tumors at 4 weeks ($n = 3$). (I) Schematic model of KIAA1429 promoting IHs regression. Scale bar: 100 μm. Statistical analyses: two-tailed unpaired Student's *t* test; $^{*}p < 0.05$, $^{**}p < 0.01$. EV, empty vector; ns, nonsignificant; shKIAA1429, KIAA1429 shRNA; shNC, normal control shRNA; OE-KIAA1429, KIAA1429 overexpression vector.

Therefore, the formation of GLUT1^{+} vessels is considered the successful criterion of IH animal models.[40,41] As a glycolysis-related protein, GLUT1 is often highly expressed in malignant tumors due to increased metabolism and glycolysis.[42] However, the high expression of GLUT1 in IHs cannot be completely explained by adaptation to metabolic changes. A previous study revealed that the expression of GLUT1 in both proliferative and involuting IHs is higher than that in normal skin, manifesting the fact that the increase in GLUT1 is not a transient adaptation to increased glycolytic demand.[38] In addition, it was also proven that there was no correlation between high expression levels of GLUT1 and Ki67, suggesting that the high expression of GLUT1 in IHs, at least in involuting and involuted IHs, is unrelated to proliferative activity.[38] These results indicated that the function of GLUT1 in IHs has not been fully elucidated.

This study also explored how KIAA1429 played a role in GLUT1. Although KIAA1429 is a member of the m^{6}A methyltransferase complex, it is not a real methyltransferase, but acts more as a scaffold that combines the main components of the 'complex' with mRNA to mediate m^{6}A modification at specific sites.[43] Therefore, unlike other typical methyltransferases, the role of KIAA1429 is not limited to m^{6}A modification.[44,45] Based on our results from RIP and the mRNA stability assay, we believe that KIAA1429 could facilitate the stemness property of HemECs without altering the m^{6}A level of GLUT1. In addition, different changes in the mRNA and protein levels of GLUT1 after KIAA1429 overexpression also indicated other possible indirect regulation of KIAA1429 on GLUT1. Furthermore, other potential targets such as *KDR* and *FN1* were also investigated and it was found that the expression changes in these factors after KIAA1429 downregulation were also independent of m^{6}A modification.

In conclusion, this study demonstrated the function of upregulated KIAA1429 in IHs regression by inducing the transition of HemECs to facultative stem cells (Figure 7I). The findings provide further insight regarding the regression mechanism of IHs and may introduce a new potential therapeutic approach for treating IHs.

AUTHOR CONTRIBUTIONS

WL, ZY, and HZ conducted the experiments. WL, WW, and LJ analyzed the data. HR, BJ, and WL designed the study. HR supervised the study. WL wrote most of the manuscript and all the authors commented on the manuscript.

ACKNOWLEDGMENTS

None.

FUNDING INFORMATION

This work was supported by the National Natural Science Foundation of China [grant no. 82172227]; and the Clinical Medical Science Innovation Program of Jinan [grant no. 202019076].

CONFLICT OF INTEREST

The authors have no conflict of interest.

ETHICS STATEMENT

Approval of the research protocol by an Institutional Reviewer Board: This study was approved by the Committee for Ethical Review of Research involving Human Subjects of Shandong Provincial Hospital.

Informed Consent: All human specimens were collected with the informed consent of guardians.

Registry and the Registration no. of the study/trial: N/A.

Animal Studies: All animal experiments were approved by the Committee for Ethics of Animal Experiments of Shandong Provincial Hospital.

ORCID

Luying Wang https://orcid.org/0000-0002-0429-1496

REFERENCES

1. Léauté-Labrèze C, Harper JI, Hoeger PH. Infantile haemangioma. *Lancet*. 2017;390(10089):85-94. doi:10.1016/S0140-6736(16)00645-0
2. Vredenborg AD, Janmohamed SR, de Laat PC, Madern GC, Oranje AP. Multiple cutaneous infantile haemangiomas and the risk of internal haemangioma. *Br J Dermatol*. 2013;169(1):188-191. doi:10.1111/bjd.12229
3. Rodríguez Bandera AI, Sebaratnam DF, Wargon O, Wong LF. Infantile hemangioma. Part 1: epidemiology, pathogenesis, clinical presentation and assessment. *J Am Acad Dermatol*. 2021;85(6):1379-1392. doi:10.1016/j.jaad.2021.08.019
4. Couto RA, Maclellan RA, Zurakowski D, Greene AK. Infantile hemangioma: clinical assessment of the involuting phase and implications for management. *Plast Reconstr Surg*. 2012;130(3):619-624. doi:10.1097/PRS.0b013e31825dc129
5. Krowchuk DP, Frieden IJ, Mancini AJ, et al. Clinical practice guideline for the Management of Infantile Hemangiomas. *Pediatrics*. 2019;143(1):e20183475. doi:10.1542/peds.2018-3475
6. Léauté-Labrèze C, Baselga Torres E, Weibel L, et al. The infantile hemangioma referral score: a validated tool for physicians. *Pediatrics*. 2020;145(4):e20191628. doi:10.1542/peds.2019-1628
7. Kowalska M, Dębek W, Matuszczak E. Infantile hemangiomas: an update on pathogenesis and treatment. *J Clin Med*. 2021;10(20):4631. doi:10.3390/jcm10204631

8. Greenberger S, Bischoff J. Pathogenesis of infantile haemangioma. *Br J Dermatol*. 2013;169(1):12-19. doi:10.1111/bjd.12435
9. Yu Y, Flint AF, Mulliken JB, Wu JK, Bischoff J. Endothelial progenitor cells in infantile hemangioma. *Blood*. 2004;103(4):1373-1375. doi:10.1182/blood-2003-08-2859
10. Huang L, Nakayama H, Klagsbrun M, Mulliken JB, Bischoff J. Glucose transporter 1-positive endothelial cells in infantile hemangioma exhibit features of facultative stem cells. *Stem Cells*. 2015;33(1):133-145. doi:10.1002/stem.1841
11. Chen XY, Zhang J, Zhu JS. The role of m^6A RNA methylation in human cancer. *Mol Cancer*. 2019;18(1):103. doi:10.1186/s12943-019-1033-z
12. Lan T, Li H, Zhang D, et al. KIAA1429 contributes to liver cancer progression through N6-methyladenosine-dependent post-transcriptional modification of GATA3. *Mol Cancer*. 2019;18(1):186. doi:10.1186/s12943-019-1106-z
13. Zhou Y, Pei Z, Maimaiti A, et al. m^6A methyltransferase KIAA1429 acts as an oncogenic factor in colorectal cancer by regulating SIRT1 in an m^6A-dependent manner. *Cell Death Discov*. 2022;8(1):83. doi:10.1038/s41420-022-00878-w
14. Xu Y, Chen Y, Yao Y, et al. VIRMA contributes to non-small cell lung cancer progression via N^6-methyladenosine-dependent DAPK3 post-transcriptional modification. *Cancer Lett*. 2021;522:142-154. doi:10.1016/j.canlet.2021.08.027
15. Zhang X, Dai XY, Qian JY, et al. SMC1A regulated by KIAA1429 in m6A-independent manner promotes EMT progress in breast cancer. *Mol Ther Nucleic Acids*. 2021;27:133-146. doi:10.1016/j.omtn.2021.08.009
16. Qian JY, Gao J, Sun X, et al. KIAA1429 acts as an oncogenic factor in breast cancer by regulating CDK1 in an N6-methyladenosine-independent manner. *Oncogene*. 2019;38(33):6123-6141. doi:10.1038/s41388-019-0861-z
17. Mulliken JB, Glowacki J. Hemangiomas and vascular malformations in infants and children: a classification based on endothelial characteristics. *Plast Reconstr Surg*. 1982;69(3):412-422. doi:10.1097/00006534-198203000-00002
18. der Sarkissian SA, Wargon O, Sebaratnam DF. International heterogeneity in admission criteria and monitoring for the initiation of propranolol in infantile hemangioma. *JAAD Int*. 2020;1(2):111-113. doi:10.1016/j.jdin.2020.06.005
19. Hoeger PH, Harper JI, Baselga E, et al. Treatment of infantile haemangiomas: recommendations of a European expert group. *Eur J Pediatr*. 2015;174(7):855-865. doi:10.1007/s00431-015-2570-0
20. Léauté-Labrèze C, Dumas de la Roque E, Hubiche T, Boralevi F, Thambo JB, Taïeb A. Propranolol for severe hemangiomas of infancy. *N Engl J Med*. 2008;358(24):2649-2651. doi:10.1056/NEJMc0708819
21. Solman L, Glover M, Beattie PE, et al. Oral propranolol in the treatment of proliferating infantile haemangiomas: british society for paediatric dermatology consensus guidelines. *Br J Dermatol*. 2018;179(3):582-589. doi:10.1111/bjd.16779
22. Marqueling AL, Oza V, Frieden IJ, Puttgen KB. Propranolol and infantile hemangiomas four years later: a systematic review. *Pediatr Dermatol*. 2013;30(2):182-191. doi:10.1111/pde.12089
23. Sans V, de la Roque ED, Berge J, et al. Propranolol for severe infantile hemangiomas: follow-up report. *Pediatrics*. 2009;124(3):e423-e431. doi:10.1542/peds.2008-3458
24. Holmes WJ, Mishra A, Gorst C, Liew SH. Propranolol as first-line treatment for rapidly proliferating infantile haemangiomas. *J Plast Reconstr Aesthet Surg*. 2011;64(4):445-451. doi:10.1016/j.bjps.2010.07.009
25. Shah SD, Baselga E, McCuaig C, et al. Rebound growth of infantile hemangiomas after propranolol therapy. *Pediatrics*. 2016;137(4):e20151754. doi:10.1542/peds.2015-1754
26. Caussé S, Aubert H, Saint-Jean M, et al. Propranolol-resistant infantile haemangiomas. *Br J Dermatol*. 2013;169(1):125-129. doi:10.1111/bjd.12417
27. Itinteang T, Withers AH, Davis PF, Tan ST. Biology of infantile hemangioma. *Biology of Infantile Hemangioma Front Surg*. 2014;1:38. doi:10.3389/fsurg.2014.00038
28. Itinteang T, Tan ST, Brasch H, Day DJ. Haemogenic endothelium in infantile haemangioma. *J Clin Pathol*. 2010;63(11):982-986. doi:10.1136/jcp.2010.081257
29. Itinteang T, Tan ST, Brasch HD, Vishvanath A, Day DJ. Primitive erythropoiesis in infantile haemangioma. *Br J Dermatol*. 2011;164(5):1097-1100. doi:10.1111/j.1365-2133.2010.10187.x
30. Itinteang T, Vishvanath A, Day DJ, Tan ST. Mesenchymal stem cells in infantile haemangioma. *J Clin Pathol*. 2011;64(3):232-236. doi:10.1136/jcp.2010.085209
31. de Jong S, Itinteang T, Withers AH, Davis PF, Tan ST. Does hypoxia play a role in infantile hemangioma? *Arch Dermatol Res*. 2016;308(4):219-227. doi:10.1007/s00403-016-1635-x
32. Ji Y, Chen S, Li K, Li L, Xu C, Xiang B. Signaling pathways in the development of infantile hemangioma. *J Hematol Oncol*. 2014;7:13. doi:10.1186/1756-8722-7-13
33. Jiang X, Liu B, Nie Z, et al. The role of m6A modification in the biological functions and diseases. *Signal Transduct Target Ther*. 2021;6(1):74. doi:10.1038/s41392-020-00450-x
34. Hou J, Zhang H, Liu J, et al. YTHDF2 reduction fuels inflammation and vascular abnormalization in hepatocellular carcinoma. *Mol Cancer*. 2019;18(1):163. doi:10.1186/s12943-019-1082-3
35. Yao MD, Jiang Q, Ma Y, et al. Role of METTL3-dependent N^6-Methyladenosine mRNA modification in the promotion of angiogenesis. *Mol Ther*. 2020;28(10):2191-2202. doi:10.1016/j.ymthe.2020.07.022
36. Dosanjh A, Chang J, Bresnick S, et al. In vitro characteristics of neonatal hemangioma endothelial cells: similarities and differences between normal neonatal and fetal endothelial cells. *J Cutan Pathol*. 2000;27(9):441-450.doi:10.1034/j.1600-0560.2000.027009441.x
37. Boye E, Yu Y, Paranya G, Mulliken JB, Olsen BR, Bischoff J. Clonality and altered behavior of endothelial cells from hemangiomas. *J Clin Invest*. 2001;107(6):745-752. doi:10.1172/JCI11432
38. North PE, Waner M, Mizeracki A, Mihm MC Jr. GLUT1: a newly discovered immunohistochemical marker for juvenile hemangiomas. *Hum Pathol*. 2000;31(1):11-22. doi:10.1016/s0046-8177(00)80192-6
39. van Vugt LJ, van der Vleuten CJM, Flucke U, Blokx WAM. The utility of GLUT1 as a diagnostic marker in cutaneous vascular anomalies: a review of literature and recommendations for daily practice. *Pathol Res Pract*. 2017;213(6):591-597. doi:10.1016/j.prp.2017.04.023
40. Khan ZA, Boscolo E, Picard A, et al. Multipotential stem cells recapitulate human infantile hemangioma in immunodeficient mice. *J Clin Invest*. 2008;118(7):2592-2599. doi:10.1172/JCI33493
41. Xu D, TM O, Shartava A, et al. Isolation, characterization, and in vitro propagation of infantile hemangioma stem cells and an in vivo mouse model. *J Hematol Oncol*. 2011;4:54. doi:10.1186/1756-8722-4-54
42. Barron CC, Bilan PJ, Tsakiridis T, Tsiani E. Facilitative glucose transporters: implications for cancer detection, prognosis and treatment. *Metabolism*. 2016;65(2):124-139. doi:10.1016/j.metabol.2015.10.007
43. Yue Y, Liu J, Cui X, et al. VIRMA mediates preferential m^6A mRNA methylation in 3'UTR and near stop codon and associates with alternative polyadenylation. *Cell Discov*. 2018;4:10. doi:10.1038/s41421-018-0019-0
44. Miao R, Dai CC, Mei L, et al. KIAA1429 regulates cell proliferation by targeting c-Jun messenger RNA directly in gastric cancer. *J Cell Physiol*. 2020;235(10):7420-7432. doi:10.1002/jcp.29645
45. Qian JY, Gao J, Sun X, et al. KIAA1429 acts as an oncogenic factor in breast cancer by regulating CDK1 in an

N6-methyladenosine-independent manner. *Oncogene*. 2019;38(33):6123-6141. doi:10.1038/s41388-019-0861-z

SUPPORTING INFORMATION

Additional supporting information can be found online in the Supporting Information section at the end of this article.

How to cite this article: Wang L, Zou Y, Huang Z, et al. KIAA1429 promotes infantile hemangioma regression by facilitating the stemness of hemangioma endothelial cells. *Cancer Sci*. 2023;114:1569-1581. doi:10.1111/cas.15708